Parallel ray tracing for radiative heat transfer

Application in a distributed computing environment

J.G. Marakis, J. Chamiço, G. Brenner and F. Durst
Institute of Fluid Mechanics, University of Erlangen-Nuremberg, Erlangen, Germany

Received December 2000
Revised May 2001
Accepted June 2001

Keywords *Radiation, Anisotropy, Monte Carlo simulation, Parallel computing, Heat transfer*

Abstract *Notes that, in a full-scale application of the Monte Carlo method for combined heat transfer analysis, problems usually arise from the large computing requirements. Here the method to overcome this difficulty is the parallel execution of the Monte Carlo method in a distributed computing environment. Addresses the problem of determination of the temperature field formed under the assumption of radiative equilibrium in an enclosure idealizing an industrial furnace. The medium contained in this enclosure absorbs, emits and scatters anisotropically thermal radiation. Discusses two topics in detail: first, the efficiency of the parallelization of the developed code, and second, the influence of the scattering behavior of the medium. The adopted parallelization method for the first topic is the decomposition of the statistical sample and its subsequent distribution among the available processors. The measured high efficiencies showed that this method is particularly suited to the target architecture of this study, which is a dedicated network of workstations supporting the message passing paradigm. For the second topic, the results showed that taking into account the isotropic scattering, as opposed to neglecting the scattering, has a pronounced impact on the temperature distribution inside the enclosure. In contrast, the consideration of the sharply forward scattering, that is characteristic of all the real combustion particles, leaves the predicted temperature field almost undistinguishable from the absorbing/emitting case.*

Nomenclature

E	= efficiency parameter
g	= asymmetry factor
$\dot{q}$	= heat source
R	= cumulative distribution function
s	= length
S	= speed-up parameter
T	= temperature
x,y,z	= coordinates
β	= extinction coefficient
ΔV	= volume
ε	= emissivity
ϑ	= polar angle
κ	= absorption coefficient
σ	= Stefan-Boltzmann constant
σ_s	= scattering coefficient
ρ	= reflectivity
φ	= azimuth angle
Φ	= phase function
ω	= scattering albedo

Subscripts

c	= conditional
e	= emission
g	= global
i	= number or ray element
L	= extinction point
m	= marginal
p	= parallel
r	= radiative
s	= scattering
v	= volumetric
w	= wall

This work was financially supported by the Commission of the European Communities under the TMR network "Fundamental improvements in radiative heat transfer – RADIARE" (CT-98-224).

Introduction

Thermal radiation is an important heat transfer mode in many manufacturing, material processing and industrial applications. In fossil fuel combustion, for example, radiative heat exchange is a significant design parameter for furnaces, combustion chambers and various types of flames. In the semiconductor industry, infra-red heat sources are used in several processes, such as the Czochralski crystal growth and chemical vapor deposition. Other well-known applications of radiative heat transfer include high temperature heat exchangers, solar energy collectors and radiant cooling used in electronic packaging and air-conditioning. In all of these applications, thermal radiation is combined with convection and conduction. The balance between these heat transfer modes is expressed through the energy equation. The iterative solution of this equation is a time-consuming procedure that is further impeded by the strong non-linearity of the radiant source term.

This difficulty motivates the present work. The objective is to solve a complete multidimensional radiative heat transfer problem, including scattering, using the accurate but time-consuming Monte Carlo method. Furthermore, the problem is formulated in the terms usually occurring in engineering practice, that is, estimation of the temperature field by solving some form of the energy equation. The problem associated with this formulation is the large requirement in computing power. This difficulty is overcome in the present work by applying the Monte Carlo method in a distributed computing environment. Then, the sufficient computational resources commonly found in these configurations are used to investigate the influence of anisotropic scattering on the radiant heat exchange within an idealized furnace.

Many methods, and numerous variants of these methods, have been developed for the solution of radiative heat transfer problems. Standard textbooks in thermal radiation (Siegel and Howell, 1992; Modest, 1993; Brewster, 1992) distinguish between the zonal (Hottel and Sarofim, 1967), the Monte Carlo (Siegel and Howell, 1992; Haji-Sheikh, 1988), the P-N or spherical harmonics (Modest, 1974, 1975; Mengüç and Viskanta, 1985, 1986), and the S-N or discrete ordinates (Fiveland, 1984; Truelove, 1988) methods, as main categories. Together with these, the discrete transfer (Lockwood and Shah, 1981; Coelho and Carvalho, 1997) and the finite volume (Raithby and Chui, 1990; Raithby, 1999) methods should be mentioned, the former because of its frequent application in combustion modeling and the latter because of its increasing acceptance. With the exception of the P-N approximation, all the previously mentioned methods have been applied in parallel computer architectures. The parallelization of the (a) zonal and (b) Monte Carlo methods has been addressed by Saltiel and Naraghi (1993) and Burns and Pryor (1989) and Farmer and Howell (1998), respectively. The same topic has been investigated for the discrete ordinates method by Gonçalves and Coelho (1997), for the discrete transfer method by Novo *et al.* (1999); Cumber and Beeri (1998)

and for the finite volume method by Liu *et al.* (1999); Coelho and Gonçalves (1999).

In all of these studies, the parallel solution is achieved using either spatial or angular decomposition. A third option, the wavelength decomposition, although the most straightforward, has not been exploited in these studies, since they all assumed gray media. The spatial decomposition has been examined by Gonçalves and Coelho (1997); Novo *et al.* (1999); Liu *et al.* (1999); and Coelho and Gonçalves (1999). It is the most desired method because of its compatibility with the decomposition usually applied in computational fluid dynamics. However, in the references cited earlier, it obtained poor parallelization efficiencies. This seems to be in accordance with the nature of thermal radiation as a potentially long-range acting phenomenon that may require intensive exchange of information between the spatial subdomains. Angular decomposition is the method that gave the best results with respect to the parallelization and speed-up efficiencies. However, its application in architectures with many processors is pronouncedly limited in the cases where the adopted radiation model has a low angular resolution.

The Monte Carlo method offers another parallelization option. This is the event or sampling parallelization, which takes advantage of the statistical nature of the method. In Monte Carlo, the radiant exchange is simulated with a sufficiently large amount of discrete elementary energy packets. Emission, absorption, scattering and reflection of these packets are represented by probability density functions, which are used to examine the history of the energy packets. Each packet is independent of the rest of the sample and therefore its history can be examined independently, simultaneously and thus in parallel with the others.

The Monte Carlo algorithm is described in the next section. The emphasis is given in presenting the innermost part of the sequential algorithm that forms the basis for the parallel implementation. This algorithm is then applied for the idealized furnace described by Mengüç and Viskanta (1985). This problem has been referenced many times in the literature, where it has been solved using either sequential approaches (Truelove, 1988; Coelho and Carvalho, 1997) or parallel radiation models (Gonçalves and Coelho, 1997; Novo *et al.*, 1999; Cumber and Beeri, 1998; Coelho and Gonçalves, 1999). For this problem, new test cases are constructed and solved. Their aim is twofold: first, to evaluate the parallel performance of the algorithm, and second, to demonstrate how the ample resources found in a parallel architecture can be used to solve a demanding problem, such as the influence of anisotropic scattering. The paper ends with a summary of the key points and the conclusions.

Formulation

Since the pioneering work of Howell and Perlmutter (1964) and Perlmutter and Howell (1964), Monte Carlo methods have found a wide range of applications in radiative heat transfer. A recent review of this subject is given by Howell (1998). Detailed descriptions of the method can be found in textbooks (Siegel

and Howell, 1992; Modest, 1993; Brewster, 1992) and monographs (Haji-Sheikh, 1988; Yang *et al.*, 1995). In this section, the computations composing a Monte Carlo algorithm will be presented, with the emphasis on the algorithmic branch dealing with anisotropic scattering and the conversion from the sequential to the parallel algorithm.

Sequential Monte Carlo algorithm

A schematic of the sequential Monte Carlo algorithm is shown in Figure 1. The input data of the algorithm are the geometric and grid information, the temperature and emissivity distributions on the boundaries, and the field distributions of the absorption coefficient, the scattering coefficient and the asymmetry factor. The initial step is to calculate the characteristics of the sample that will be examined for each volume or surface element. For that purpose, either the amount of energy packets or the energy carried by each packet is prescribed and the remaining undefined quantity is determined after calculating the thermal power emitted by each spatial element. Then a set of energy packets is emitted and their propagation history within the enclosure is recorded. This is done in the inner loop shown in Figure 1.

The inner loop is repeated as many times as it takes either to make the maximum local standard deviation of the radiative source term fall below a prescribed limit, or to make the number of iterations exceed a prescribed value. The use of the standard deviation as a measure of the error introduced by the statistical nature of the Monte Carlo method is a simple and generally applicable approach. The disadvantage of this approach is the high computation cost that is created by the repetition of the same simulation. More elaborate methods for controlling the convergence of Monte Carlo methods have been proposed by Kobiyama (1989) and Schweiger *et al.* (1999). These approaches refer to iterative applications of a Monte Carlo method in a combined heat transfer problem. They are based on the reuse of the information generated by a previous set of energy packets that may lead to significant savings in computer time. However, the efficient parallelization of these approaches is a topic that demands future investigation.

The inner loop of the algorithm traces each of the emitted energy packets. The preliminary steps to initiate this tracing are the random selections of the emission point, the extinction optical length and the emission direction. The first step is done by considering the probability of each emission point as homogeneously distributed within each spatial element. For the second step, a value between 0 and 1 is assigned to the extinction random variable R_s. The use of this variable will be discussed later. The third step, the choice of the emission direction, is done by specifying the azimuth φ and the polar ϑ angles. Both angles refer to a relative system of axes attached and carried by the energy packet. Transformations between this relative and the absolute system are made using a rotation matrix. The cumulative distribution functions (cdfs) for the random selection of the polar and the azimuth angles are shown in Table I.

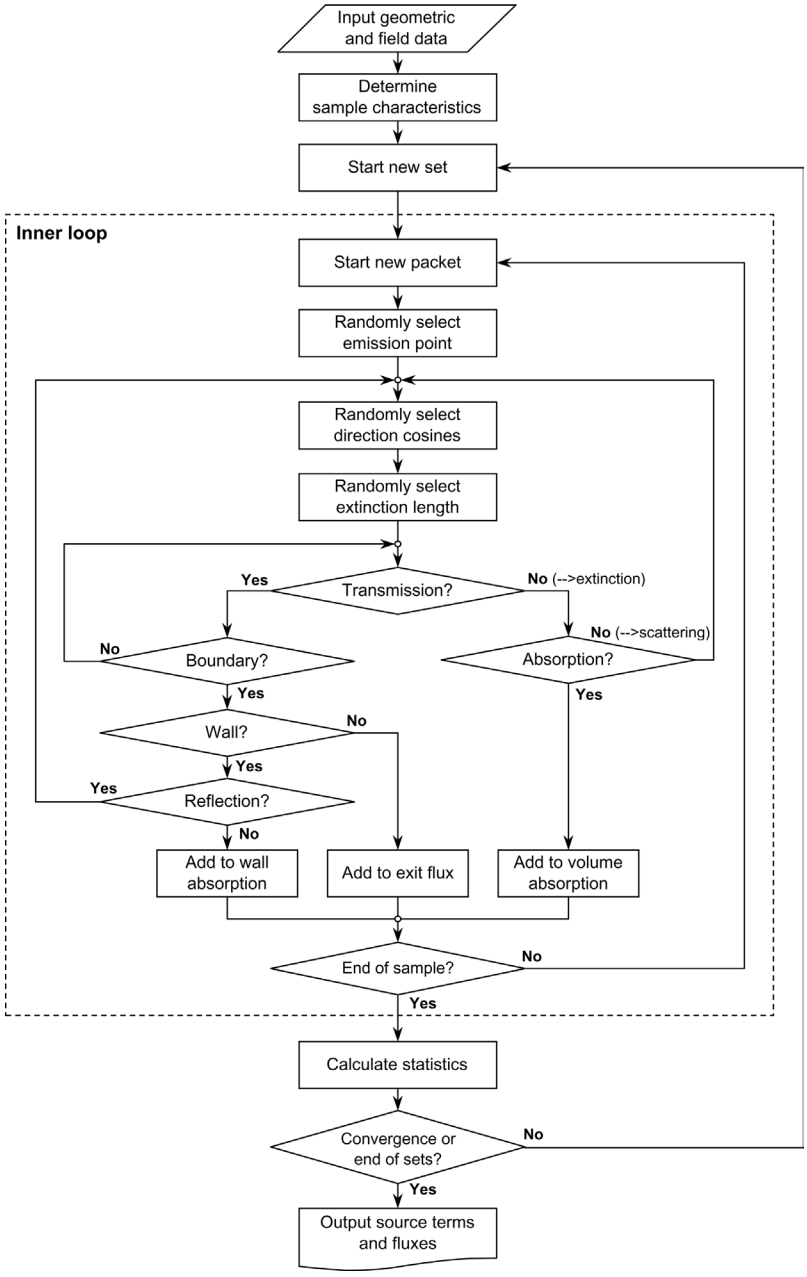

Figure 1.
Sequential Monte Carlo algorithm. The inner loop remains unchanged in the parallel version

After the emission direction has been chosen, a simple algorithmic procedure defines the intersection points between this direction and the bounding surfaces of the control volumes. In each successive intersection, the condition whether $\ln R_s + \sum_i s_i \beta_i > 0$ is examined. In this expression, s_i is the length traveled within the currently traced control volume and β_i is the corresponding

extinction coefficient. If this condition holds, the next intersection point is calculated until a boundary is reached; otherwise the extinction point L is defined such that

$$\ln R_s + \sum_{i=1}^{L-1} s_i \beta_i + s_L \beta_L = 0 \tag{1}$$

Extinction at point L should be interpreted either as absorption, or scattering. This is done by comparing the value of a random variable R_ω with the value of the local scattering albedo ω. If absorption occurs, then the energy carried by the packet is tallied on the corresponding accumulator and the control is brought to the point where the decision is made whether to inject a new packet or to stop, because the end of the sampling set has been reached. The second option for an extinction event is scattering. This is interpreted as absorption and simultaneous anisotropic re-emission. The cdf for the choice of the azimuth and polar angles of the after-scattering direction is directly related to the phase function $\Phi(\vartheta, \varphi)$ of the medium

$$R(\vartheta, \varphi) = \int_0^{\varphi} \int_0^{\vartheta} \Phi(\vartheta, \varphi) \sin \vartheta d\vartheta d\varphi \tag{2}$$

In general, the phase function depends on both the azimuthal and polar angles and therefore equation (2) is a joint cdf which should be decomposed into appropriate marginal and conditional functions in order to sample the scattering angles. The problem is significantly simplified if the phase function has an azimuthal symmetry. In this case a marginal cdf for the azimuth angle is directly derived from equation (2) as

$$R_{m,\varphi} = \int_0^{\varphi} \int_0^{\pi} \Phi(\vartheta) \sin \vartheta d\vartheta d\varphi = \frac{\varphi}{2\pi} \tag{3}$$

The conditional cdf for the polar angle that corresponds to equation (3) is then

Parameter	Phenomenon	Function
ϕ	Emission from surface and volume, reflection, scattering	$\varphi = 2\pi R_\varphi$
	Emission from surface and reflection	$\vartheta = \sin^{-1}\left(\sqrt{R_\vartheta}\right)$
ϑ	Emission from volume	$\vartheta = \cos^{-1}(1 - 2R_\vartheta)$
	Scattering	$\vartheta = \cos^{-1}\left(\left(1 + g^2 - \left(\frac{1-g^2}{1+2gR_\vartheta - g}\right)^2\right)/2g\right)$

Table I.
Cumulative distribution functions for direction sampling

$$R_{c,\vartheta|\varphi} = \frac{\int_0^{\varphi}\int_0^{\vartheta}\Phi(\vartheta)\sin\vartheta d\vartheta d\varphi}{R_{m,\varphi}} = \int_0^{\vartheta}\Phi(\vartheta)\sin\vartheta d\vartheta \tag{4}$$

In the case where the scattering particles are spherical, homogeneous and isotropic, the phase function $\Phi(\vartheta)$ can be rigorously determined by applying the Lorenz-Mie theory of elastic scattering (Bohren and Huffman, 1983). This approach has been followed by Marakis *et al.* (2001). However, the use of the Lorenz-Mie phase function has two disadvantages; first, it increases significantly the computational effort because of the associated lengthy calculations, and, second, its introduction into equation (4) does not lead to a closed form for sampling the polar angle. The latter problem has been overcome by Marakis *et al.* (2001) by creating a look-up table containing the values of the phase function in a prescribed grid of angular positions and then interpolating for intermediate values of the polar angle. However, this procedure creates a significant computational overhead. In the present study, the Henyey-Greenstein phase function is adopted:

$$\Phi(\vartheta) = \frac{1-g^2}{(1+g^2-2g\cos\vartheta)^{3/2}} \tag{5}$$

In equation (5), g is the asymmetry factor of the medium. This parameter is defined as the integral of the phase function over the solid angle and thus it can be rigorously determined using the Lorenz-Mie solution. However, in most practical situations, the asymmetry factor is averaged over the Planck function and a particle size distribution and therefore only mean values characteristic of the kind of scattering particles are of interest. The Henyey-Greenstein expression has been tested against the rigorous Lorenz-Mie phase function by Gouesbet *et al.* (1983). It was found to represent satisfactorily the strong forward scattering of combustion particles. In the context of the present study, the main advantage of equation (5) is that it turns equation (4) into an expression appropriate for the direct sampling of the polar angle

$$\vartheta = \cos^{-1}\left(\left(1+g^2-\left(\frac{1-g^2}{1+2gR_{\vartheta}-g}\right)^2\right)\Big/2g\right) \tag{6}$$

With reference to Figure 1, the branch that completes the inner loop refers to the possibility that the propagating packet reaches a boundary. This possibility is treated conventionally by considering three options; diffuse reflection using the cdfs of Table I, wall absorption, or exit from the computational domain.

Parallel Monte Carlo algorithm

The concept followed for the parallelization of the Monte Carlo method is to trace concurrently as many energy packets as the available computing nodes. This is schematically shown in Figure 2. The building-block for the parallel

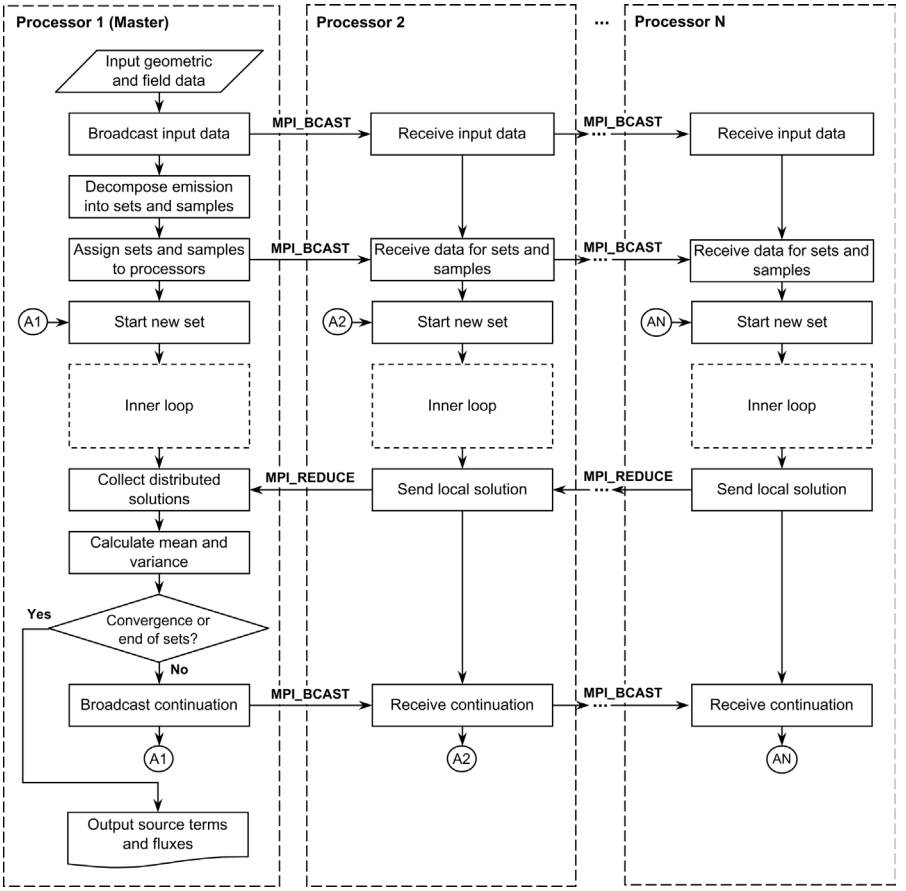

Figure 2.
Parallel Monte Carlo algorithm. The communication between the processors has been implemented using the message passing interface (MPI)

algorithm is the inner loop shown in Figure 1. This loop remains unchanged in the parallel version. The difference here is that each sample is further decomposed into N_p subsets, where N_p is the number of the active processors. This concept is a direct implementation of the single-program-multiple-data paradigm. According to this programming model, the same code is executed in each node but processes different portions of data, i.e. traces different energy packets. The algorithm has been implemented using the message passing interface (MPI). A very similar implementation would have been obtained if another message passing library had been used.

The algorithm starts by choosing one processor to be the master. This master node performs the input task and broadcasts the geometric and field data to the client processors. If the processors are of the same computing power, the number of energy packets that will be examined in each node equals the sample size divided by N_p. In the case of a non-homogeneous architecture, the effectiveness of this simple balancing scheme can be maintained by introducing a set of weighting factors depending on the computing power per node. After completion

of the calculations for each set, information about the absorbed amount of energy per volume or surface element that is distributed among the processors is collected back to the master node. The algorithm then checks whether any of the termination criteria are met and broadcasts this information to the clients.

The target architecture for the implementation of this algorithm is a dedicated network of computers. There are a few reasons that make this architecture suitable for the adopted parallelization method and vice versa. The first reason is that it may require a considerable amount of memory per node, because all the spatial information (geometry, field data and boundary conditions) should be stored locally. This requirement is easily met in the dedicated network architecture, since each node can be easily equipped with a sufficient amount of memory. The second reason is that the histories of the energy packets are by definition independent and therefore only the statistics of a sampling set have to be transferred among the processors. This minimal communication requirement between the nodes helps to avoid any potential network bottleneck caused by limited network bandwidth. Furthermore, even if the network is non-homogeneous, the load balancing is much simpler compared with the domain decomposition method, because the only adjustable parameter is the size of the sample that is processed by each node.

Results

The algorithm presented in the previous section is applied to study the radiant heat transfer in the three-dimensional furnace-like enclosure examined by Mengüç and Viskanta (1985). The dimensions of this idealized furnace are $2 \times 2 \times 4$m in the *x, y, z* directions, respectively. The temperature and the emissivity are 1,200K and 0.85 for the bottom wall, 400K and 0.7 for the top wall, while, for the peripheral walls, $T_w = 900$K and $\varepsilon_w = 0.7$. These data will be kept constant for all the cases that will be examined below.

The varying parameters are summarized in Table II. The test cases shown there can be classified in three categories. In the first category belong cases 1 and 2, where the medium only absorbs and emits. These cases serve for code validation by comparing the Monte Carlo results with the zone calculations of

Category	Case	β(m^{-1})	ω(-)	g(-)	Grid
Code validation	1	0.5	0.0	–	$7 \times 7 \times 12$
	2	0.5	0.0	–	$12 \times 12 \times 22$
Influence of scattering	3	0.5	0.7	0.0	$12 \times 12 \times 22$
	4	0.5	0.7	0.9	$12 \times 12 \times 22$
	5	0.85	0.41	0.9	$12 \times 12 \times 22$
Parallel performance	6	0.5	0.0	–	$12 \times 12 \times 22$
	7	0.5	0.0	–	(a) $7 \times 7 \times 12$ (b) $12 \times 12 \times 22$ (c) $22 \times 22 \times 42$

Table II. Specifications of the examined test cases

Mengüç and Viskanta (1985). In the second category belong cases 3-5, where scattering is modeled. The aim of this category is to investigate the validity of assumptions commonly adopted in engineering calculations, such as neglecting of scattering, or consideration of isotropic, instead of anisotropic, scattering. In the third category belong test cases 6 and 7, which are concerned with the performance evaluation of the parallel ray-tracing method.

For convenience, all of the seven cases assume gray and spatially constant radiative properties. These two assumptions do not influence the parallelization efficiency of the ray-tracing algorithm. Calculations with spectrally dependent and spatially varying properties using the serial version of this code are cited in Marakis *et al.* (2000, 2001). As indicated by equation (1), the parallel ray-tracing version runs as if the medium has spatially varying properties.

Medium in radiative equilibrium

In cases 1-5 the calculated quantities are the temperature field and the wall fluxes. The former is estimated through an energy balance between the emitted and the absorbed amount of energy and the heat source. That implies an iterative procedure, according to which the temperature is updated for every control volume as

$$T_{new}^4 = T_{old}^4 + \frac{1}{4\kappa\sigma}(\dot{q}_v - \dot{q}_r) \tag{7}$$

In equation (7), $\dot{q}_v$ is the volumetric heat source, taken constant and equal to 5kW/m^3 in all cases, and $\dot{q}_r$ is the volumetric radiative source term calculated by the Monte Carlo method. The iteration begins with an initial guess of the temperature field and continues until the maximum local temperature difference with the previous value falls below a prescribed value. This control of the temperature convergence is the only additional item in the algorithm shown in Figure 2. Equation (7) is highly non-linear and for that reason strong under-relaxation is usually necessary to solve it.

The results for the absorbing and emitting medium are shown in Figure 3. In case 1 the grid had $7 \times 7 \times 12$ elements, same as the grid of the reference zonal results. In case 2, the amount of volume elements was doubled for each direction leading to an arrangement of $12 \times 12 \times 22$ elements. In the initial and intermediate iterations, the emitted radiant energy of each control volume was subdivided into 10^5 energy packets. In the last few iterations this amount was increased by a factor ranging from 4 to 8. This adaptation was done in order to allow the considerably faster approach towards the converged temperature field and then to smooth the temperature fluctuations caused by the statistical nature of the method. As shown in Figure 3, the agreement between the zonal results and the two Monte Carlo solutions is satisfactory. This observation applies for both the temperature field and the wall fluxes. Furthermore, the effect of the grid size is shown to be minor, with the exception of the volumes which are most strongly cooled near the periphery of the top wall, where the effect is moderate.

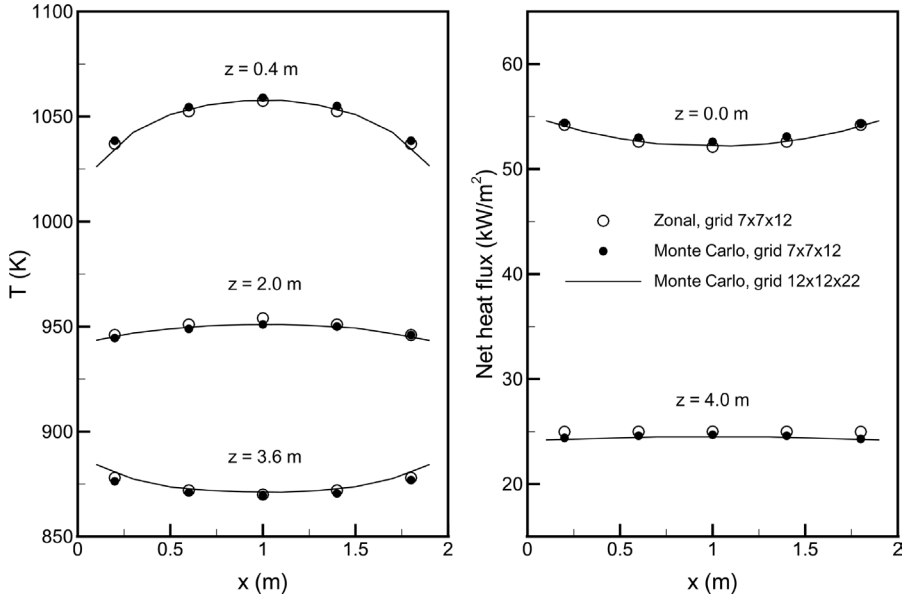

Figure 3.
Temperature (left) and net wall flux (right) distributions for cases 1 and 2. The reported values correspond to y = 1.0m. The zonal results are due to Mengüç and Viskanta (1985)

The results for the isotropic scattering case 3 are shown in Figures 4 and 5. The objective for examining this case was twofold; first, to validate the part of the algorithm that handles scattering against the results reported by Mengüç and Viskanta (1985), and second, to provide a comparison reference for the anisotropic test cases that will follow. The results between the zone and the Monte Carlo methods are again practically indistinguishable. Compared with the previous non-scattering cases, the temperature levels are higher, while the fluxes at the cold and hot walls remain practically constant. Despite these observations, case 3 is not suitable for drawing firm conclusions about the influence of scattering on the temperature distribution. The reason is that, in order to compare Monte Carlo with the zonal results of Mengüç and Viskanta (1985), their extinction coefficient was retained, while the scattering albedo was increased to 0.7. This combination corresponds to $\kappa = 0.15\text{m}^{-1}$, a value that is significantly lower than $\kappa = 0.5\text{m}^{-1}$, which was adopted in cases 1 and 2. The reduced absorption coefficient affects both the amount of energy emitted by each volume $\dot{q}_e = 4\kappa\sigma T^4 \Delta V$, and the absorption of the radiation emitted by the surrounding volume and surface elements. That obscures the prediction of the balance between these two terms and the volumetric heat source from which the temperature is derived.

Isotropic scattering is an assumption that is commonly adopted in modeling the radiant heat exchange in coal-fired furnaces. The aim of investigating the next two cases is to decide how realistic this assumption is. In case 4, the extinction coefficient and the scattering albedo remain the same as in case 3. The results are shown in Figures 4b and 5b. It can be observed in the latter Figure that the wall fluxes are higher than the isotropic case. This is explained

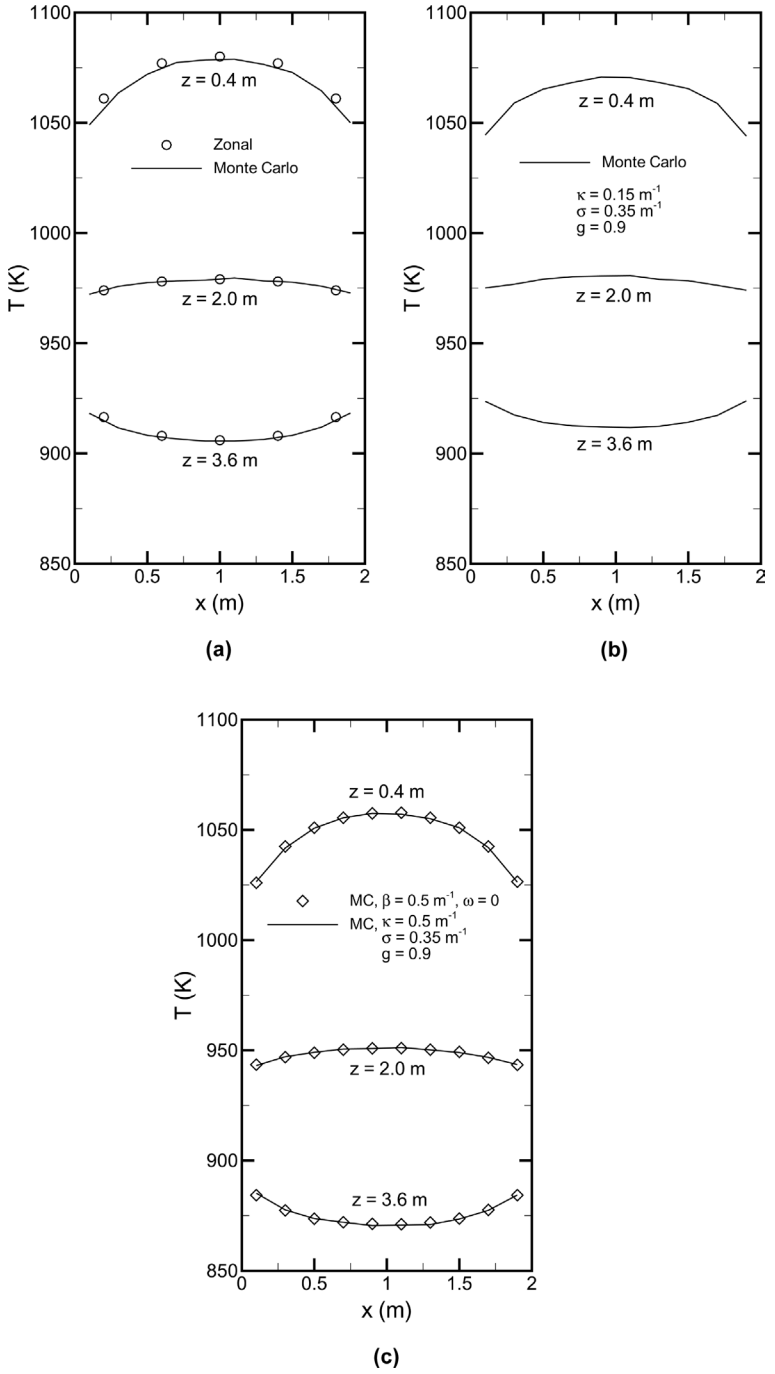

Figure 4.
Temperature distributions for (a) case 3, (b) case 4, and (c) case 5. The reported values correspond to y = 1.0m. The zonal results are due to Mengüç and Viskanta (1985)

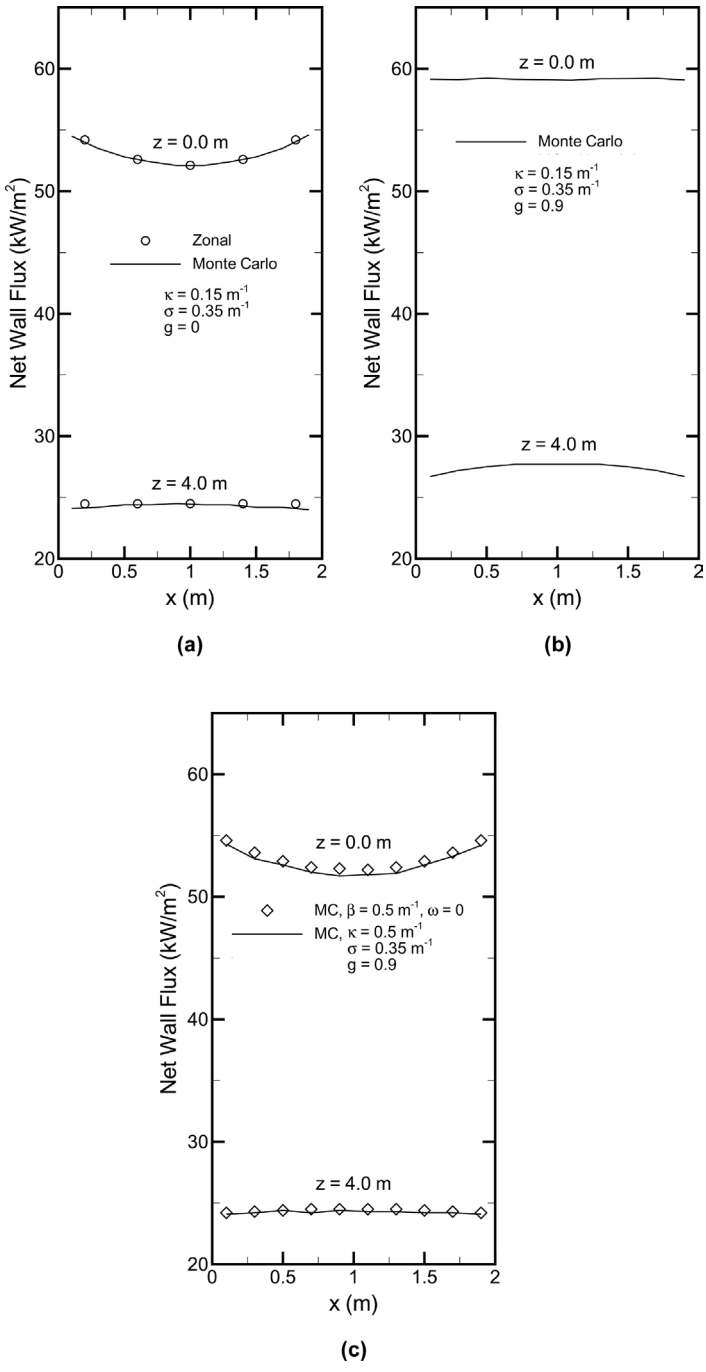

Figure 5.
Net wall flux distributions for (a) case 3, (b) case 4, and (c) case 5. The reported values correspond to y = 1.0m. The zonal results are due to Mengüç and Viskanta (1985)

by the reduction of the radiant heat flux that is back-scattered towards the interior of the enclosure. The temperature field in this case is slightly more uniform compared with case 3. In terms of the Monte Carlo method, scattering enhances absorption due to the increase of the length traveled by the energy packets within a control volume. Near the hot wall, this enhanced absorption is counterbalanced by increased emission, which is obtained by the adjustment of the temperature at a higher level. In the vicinity of the cold wall, heat is absorbed more effectively in the isotropic case, and therefore the medium temperature tends to equalize the wall temperature. However, the temperature differences between cases 3 and 4 are minor. That happens even though the examined values of the asymmetry factor represent the two opposite extremes in the scattering behavior of the particles, where for $g = 0$ any effect of scattering is maximized and for $g = 0.9$ this effect is almost cancelled. This observation questions the importance of scattering as a heat transfer mechanism.

To clarify this issue, case 5 is examined. In this case the scattering coefficient and the asymmetry factor remain the same as in case 4, while the absorption coefficient is taken as $\kappa = 0.5\text{m}^{-1}$, the same as in case 2. That matches the emission thermal power for these two cases. As shown in Figures 4c and 5c, the temperature differences between case 2 and case 5 are in the same order of magnitude as the statistical fluctuations of the Monte Carlo method. A similar observation holds for the upper wall flux, shown in Figure 5c, while the differences on the bottom wall, though systematic, are rather insignificant. It can therefore be concluded that, for conditions similar to those examined in this section, neglecting scattering is a better engineering simplification of the real anisotropic behavior of coal combustion particles than the assumption of isotropic scattering.

Parallel performance

The strategy adopted for the parallelization of the Monte Carlo method does not influence the convergence of the temperature field calculated through equation (7). That happens because the total amount of the traced energy packets per spatial element and iteration does not depend on the number of the active processors. For that reason, the test cases that will be examined in this section do not refer to an iterative solution of equation (7), as in the previous section, but instead they correspond to one global iteration which obtains the radiative source term distribution.

Three indices are used to evaluate the parallel efficiency. The first one is the speed-up factor defined as $S_p = t_1/t_p$, where t_1 and t_p are the wall clock execution times using 1 and p nodes, respectively. This factor is a direct estimate of the reduction in execution time achieved by a particular parallel algorithm. It is closely related to the second index, the global efficiency, which is defined as $E_g = t_1/(t_p p)$. The degradation of the global efficiency at higher number of processors, a problem almost synonymous with parallelization, is usually attributed to two reasons; ineffective load balancing introducing

processor latency and increased communication overhead. A direct measure of the latter is the third index, the parallel efficiency $E_p = \frac{t_{calc}}{t_{tot}}$, which is defined as the ratio of the actual calculation time over the total time spent on an iteration. In this definition, the total time t_{tot} is the sum of t_{calc} and t_{comm}, the times spent on calculation and communication, respectively.

Case 6 was run to determine the relation between the number of processors and the size of a subset. In this case, the overall amount of energy packets traced for each volume or surface element is decomposed into subsets of 500, 5,000 and 50,000 packets. The decrease of the subset size means more often calculation of the local mean radiative source term and its corresponding standard deviation. On the one hand, this is desirable because it helps to avoid unnecessary calculations after a certain level of confidence has been reached. On the other hand, the frequent collection of the sampled quantities from the distributed processors by the master processor creates a certain communication overhead. In addition, during the calculation of the statistics only the master processor is active. The effect of the subset size is shown in Figures 6a to 6c, where the speed-up factor, the global and the parallel efficiencies are plotted for runs with one to nine processors. The aggregation of data after tracing only 500 packets created a pronounced communication overhead. The speed-up and the efficiencies for 5,000 packets are acceptable for up to nine processors, while the implementation of this algorithm in a network with more computing nodes may take advantage of a greater subset size.

Case 7 was examined to determine the influence of the grid fineness. This parameter may affect directly the overall execution time not only because the total sample size per iteration is proportional to the amount of volume and surface elements, but also because the time to trace an individual packet is longer in a finer grid. For this test case, the subset size was kept constant to 50,000 packets and three progressively finer grids were examined. The speed-up was almost linear, as shown in Figure 7, while the global and the parallel efficiencies were found to be higher than 99.5 per cent for all the examined combinations of grid size and number of processors. That happens because the communication time increases only very slightly with the grid fineness and, in any case, with significantly lower rate than the calculation time.

Other parameters influencing the parallel performance of the Monte Carlo algorithm are the wall reflectivity and the scattering coefficient. These parameters were examined, but they will be only briefly reported here because they all exhibit a tendency very similar to that observed in the previous case; any prolongation of the average time to complete the tracing of an energy packet has a positive impact on the parallelization efficiency. The latter, in addition, is satisfactory in all the cases. Specifically, the parallel efficiency for nine processors and 5,000 packets per subset was measured to range between 94.9 per cent, for a $7 \times 7 \times 12$ grid and $\varepsilon_w = 1.0$, and 99.9 per cent, for a grid of $22 \times 22 \times 42$ elements and $\varepsilon_w = 0.3$. Similarly, E_p was found to be equal to 99.8 per cent, for $\omega = 0.0$, and 99.9 per cent, for $\omega = 0.7$, both cases run in nine processors and sharing a $12 \times 12 \times 22$ grid and 50,000 packets per subset. For

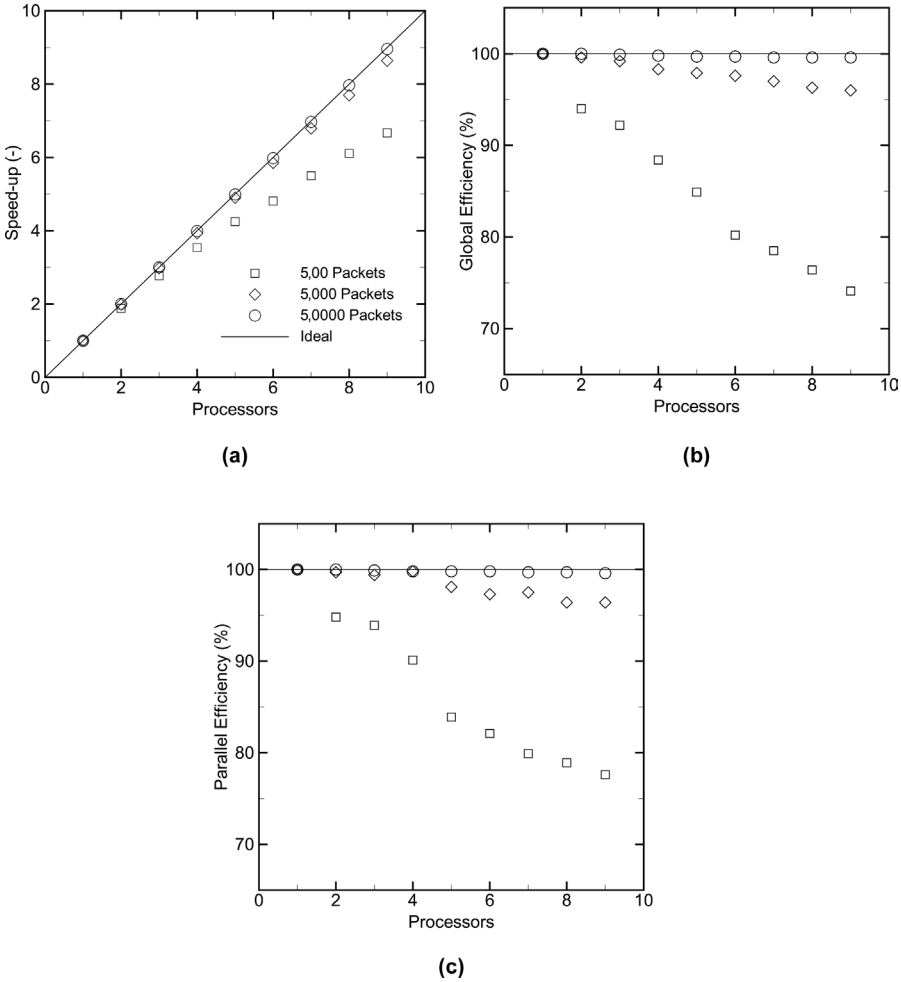

Figure 6.
Case 6; influence of the sample size on (a) speed-up; (b) global efficiency; (c) parallel efficiency

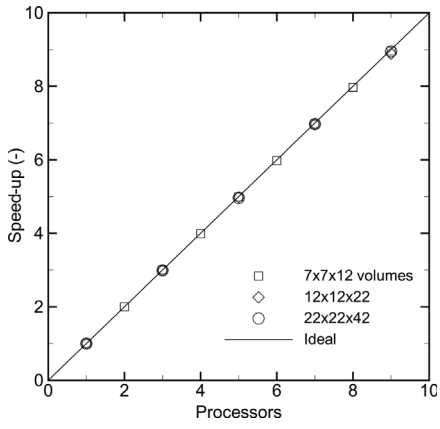

Figure 7.
Case 7; influence of the grid size on speed-up

the asymmetry factor, the expected tendency for the parallel efficiency is to increase in media with more isotropic scattering behavior. All the cases were run on a dedicated cluster made up of nine Pentium II (300MHz) processors. For case 6, the actual execution times can be derived from Figure 6 and the execution time on a single processor, which was 2,350 sec. The corresponding single-processor times for the three grids examined in case 7 were 333, 2,350, and 20,980 sec, respectively.

Conclusions

A Monte Carlo method was applied in the present study to calculate the radiant heat exchange in a furnace-like enclosure. The objective was to demonstrate the application of this method in an engineering problem that requires a significant amount of computing power. The investigated problem was the influence of anisotropic scattering on the temperature field corresponding to the equilibrium between the radiative source term and a volumetric heat source.

The code was successfully validated against data available in the literature. Then a series of new test cases was examined. It was shown that isotropic scattering has a pronounced impact on the formation of the temperature field. In contrast, when anisotropic scattering with realistic high value of the asymmetry factor was considered, the results were almost undistinguishable from the corresponding case with neglected scattering. This is an indication that the importance of scattering as a heat transfer mechanism inside furnaces may have been overestimated in previous studies. Therefore, for particles characterized by high values of the asymmetry factor, the neglecting of scattering is the suggested engineering approximation instead of the consideration of isotropic behavior.

The adopted parallelization method was the decomposition of the sample set to the available processors. This method can be characterized as intuitive; it is, however, very efficient and it may take advantage of the computing power that is readily available in almost every laboratory. Results were presented for up to nine processors. With the exception of very small sampling sets, the indices used to quantify the parallel efficiency were very high for all the examined cases. This observation indicates that an application of the parallel Monte Carlo algorithm in a computer with an order of magnitude of more processors is feasible.

References

Bohren, C.F. and Huffman, D.R. (1983), *Absorption and Scattering of Light by Small Particles*, Wiley, New York, NY.

Brewster, M.Q. (1992), *Thermal Radiative Transfer and Properties*, Wiley, New York, NY.

Burns, P.J. and Pryor, D.V. (1989), "Vector and parallel Monte Carlo radiative heat transfer simulation", *Numerical Heat Transfer*, Part B, Vol. 16, pp. 97-124.

Coelho, P.J. and Carvalho, M.G. (1997), "A conservative formulation of the discrete transfer method", *Journal of Heat Transfer*, Vol. 119, pp. 118-28.

Coelho, P.J. and Gonçalves, J. (1999), "Parallelization of the finite volume method for radiation heat transfer", *International Journal of Numerical Methods for Heat & Fluid Flow*, Vol. 9, pp. 388-404.

Cumber, P.S. and Beeri, Z. (1998), "A parallelization strategy for the discrete transfer radiation model", *Numerical Heat Transfer*, Part B, Vol. 34, pp. 287-302.

Farmer, J.T. and Howell, J.R. (1998), "Comparison of Monte Carlo strategies for radiative transfer in participating media", in Hartnett, J.P. and Irvine, T. (Eds), *Advances in Heat Transfer*, Vol. 31, Academic Press, San Diego, CA, pp. 1-97.

Fiveland, W.A. (1984), "Discrete-ordinates solutions of the radiative transport equation for rectangular enclosures", *Journal of Heat Transfer*, Vol. 106, pp. 699-706.

Gonçalves, J. and Coelho, P.J. (1997), "Parallelization of the discrete ordinates method", *Numerical Heat Transfer*, Part B, Vol. 32, pp. 151-73.

Gouesbet, G., Grehan, G. and Maheu, B. (1983), "Single scattering characteristics of volume elements in coal clouds", *Applied Optics*, Vol. 22, pp. 2038-50.

Haji-Sheikh, A. (1988), "Monte Carlo methods", in Minkowycz, W.J., Sparrow, E.M., Schneider, G.E. and Pletcher, R.H. (Eds), *Handbook of Numerical Heat Transfer*, Wiley, New York, NY.

Hottel, H.C. and Sarofim, A.F. (1967), *Radiative Transfer*, McGraw-Hill, New York, NY.

Howell, J.R. (1998), "The Monte Carlo method in radiative heat transfer", *Journal of Heat Transfer*, Vol. 120, pp. 547-60.

Howell, J.R. and Perlmutter, M. (1964), "Monte Carlo solution of thermal transfer through radiant media between gray walls", *Journal of Heat Transfer*, Vol. 86, pp. 116-22.

Kobiyama, M. (1989), "Reduction of computing time and improvement of convergence stability of the Monte Carlo method applied to radiative heat transfer with variable properties", *Journal of Heat Transfer*, Vol. 111, pp. 135-40.

Liu, J., Shang, H.M. and Chen, Y.S. (1999) "Parallel simulation of radiative heat transfer using an unstructured finite-volume method", *Numerical Heat Transfer*, Part B, Vol. 36, pp. 115-37.

Lockwood, F.C. and Shah, N.G. (1981), "A new radiation solution method for incorporation in general combustion procedures", *18th Symposium (International) on Combustion*, The Combustion Institute, pp. 1405-14.

Marakis, J.G., Brenner, G. and Durst, F. (2001), "Monte Carlo simulation of a nephelometric experiment", *International Journal of Heat and Mass Transfer*, Vol. 44, pp. 989-98.

Marakis, J.G., Papapavlou, C. and Kakaras, E. (2000), "A parametric study of radiative heat transfer in pulverised coal furnaces", *International Journal of Heat and Mass Transfer*, Vol. 43, pp. 2961-71.

Mengüç, M.P. and Viskanta, R. (1985), "Radiative transfer in three-dimensional rectangular enclosures containing inhomogeneous, anisotropically scattering media", *Journal of Quantitative Spectroscopy and Radiative Transfer*, Vol. 33, pp. 533-49.

Mengüç, M.P. and Viskanta, R. (1986), "Radiative transfer in axisymmetric, finite cylindrical enclosures", *Journal of Heat Transfer*, Vol. 108, pp. 271-6.

Modest, M.F. (1974), "Two-dimensional radiative equilibrium of a gray medium in a plane layer bounded by gray non-isothermal walls", *Journal of Heat Transfer*, Vol. 96, pp. 483-8.

Modest, M.F. (1975), "Radiative equilibrium in a rectangular enclosure bounded by gray non-isothermal walls", *Journal of Quantitative Spectroscopy and Radiative Transfer*, Vol. 15, pp. 445-61.

Modest, M.F. (1993), *Radiative Heat Transfer*, McGraw-Hill, New York, NY.

Novo, P.J., Coelho, P.J. and Carvalho, M.G. (1999), "Parallelization of the discrete transfer method", *Numerical Heat Transfer*, Part B, Vol. 35, pp. 137-61.

Perlmutter, M. and Howell, J.R. (1964), "Radiant transfer through a gray gas between concentric cylinders using Monte Carlo", *Journal of Heat Transfer*, Vol. 86, pp. 169-79.

Raithby, G.D. (1999), "Discussion of the finite-volume method for radiation, and its application using 3D unstructured meshes", *Numerical Heat Transfer*, Part B, Vol. 35, pp. 389-405.

Raithby, G.D. and Chui, E.H. (1990), "A finite-volume method for predicting radiant heat transfer in enclosures with participating media", *Journal of Heat Transfer*, Vol. 112, pp. 415-23.

Saltiel, C. and Naraghi, M.H.N. (1993), "Parallel processing approach for radiative heat transfer prediction in participating media", *Journal of Thermophysics and Heat Transfer*, Vol. 7, pp. 739-42.

Schweiger, H., Oliva, A., Costa, M. and Pérez Segarra, C.D. (1999), "A Monte Carlo method for the simulation of transient radiation heat transfer: application to compound honeycomb transparent insulation", *Numerical Heat Transfer*, Part B, Vol. 35, pp. 113-36.

Siegel, R. and Howell, J.R. (1992), *Thermal Radiation Heat Transfer*, 3rd ed., Taylor & Francis, Washington DC.

Truelove, J.S. (1988), "Three-dimensional radiation in absorbing-emitting-scattering media using the discrete-ordinates approximation", *Journal of Quantitative Spectroscopy and Radiative Transfer*, Vol. 39, pp. 27-31.

Yang, W.J., Tanigushi, H. and Kudo, K. (1995), "Radiative heat transfer by the Monte Carlo method", in Hartnett, J.P. and Irvine, T. (Eds), *Advances in Heat Transfer*, Vol. 27, Academic Press, San Diego, CA, pp. 1-215.